

BCSJ Award Article

Photoinduced Electron Transfer of Dialkynyldisilane-Linked Zinc Porphyrin–[60]Fullerene Dyad

Hayato Tsuji,*[1,†] Mikio Sasaki,[2] Yuki Shibano,[1] Motoki Toganoh,[1] Takeshi Kataoka,[1] Yasuyuki Araki,[2] Kohei Tamao,*[1,††] and Osamu Ito*[2]

[1]International Research Center for Elements Science (IRCELS), Institute for Chemical Research, Kyoto University, Uji, Kyoto 611-0011

[2]Institute of Multidisciplinary Research for Advanced Materials, Tohoku University, Katahira, Aoba-ku, Sendai 980-8577

Received November 15, 2005; E-mail: tsuji@scl.kyoto-u.ac.jp

A zinc porphyrin–fullerene dyad with a disilane as a σ-conjugated linker has been newly synthesized to evaluate the electron transfer ability of the oligosilane chain. Its photoinduced processes have been studied using the time-resolved fluorescence and absorption measurements. Photoexcitation of the dyad causes the energy and/or electron transfer from the excited singlet state of the ZnP to C_{60} moiety in polar solvents. The charge separation takes place as a final step in the excited-state process to yield the radical-ion pair with a radical cation on the zinc porphyrin and a radical anion on the fullerene, similar to other porphyrin–fullerene dyads. Its lifetime has been estimated to be 0.43–0.52 μs on the basis of the decay rate of the fullerene radical anion in polar solvents.

A variety of donor–acceptor-linked molecules and supramolecules has been prepared to study the intramolecular photoinduced electron transfer (ET) aimed at the construction of artificial photosynthetic systems.[1] In particular, intramolecular photoinduced ET processes in porphyrinoid–fullerene-linked systems[2] have been extensively studied during the past decade. It has been demonstrated that the photoexcitation of the well-designed porphyrinoid–fullerene molecules causes fast electron transfer from the porphyrinoid to the fullerene to afford long lifetime charge-separated states,[3,4] which are favorable for the subsequent ET to other chromophores or electrodes. Porphyrins and related compounds are quite appropriate as electron donors and photosensitizers that can mimic the natural photosynthetic systems, in which these expanded π-electron systems work as efficient light-harvesting pigments as well as the donors during the early stage of the ET processes.[5] Fullerenes, such as C_{60}, are regarded as good electron acceptors and photosensitizers,[6–8] because they exhibit some advantageous features over other acceptors as follows. (1) Fullerenes have absorptions over a wide visible-region range. (2) A long lifetime excited triplet state ($^3C_{60}$*), from which the efficient ET takes place to form the radical anion species ($C_{60}^{\bullet-}$) in the presence of electron donors, is generated by an efficient intersystem crossing from the excited singlet state ($^1C_{60}$*). (3) The resulting $C_{60}^{\bullet-}$ exhibits a characteristic transient absorption band in the 1000–1100 nm region so that it is easy to detect its generation and to trace the excited dynamics. (4) The small reorganization energy λ of C_{60}[9,10] accelerates the forward ET process and decelerates the back ET process.[11] According to the Marcus theory, another important factor is the electronic coupling V that controls the ET processes, which depends not only on the donor–acceptor distance, but also on the electronic properties of the linker. Thus, extensive studies have been carried out to prepare the porphyrinoid–fullerene hybrid molecules with a variety of linkers. For example, σ-carbon-based linkers, such as amides,[6,12–15] imides,[16] and norbornylogous bridges,[17] show a large attenuation factor for the electronic coupling, while π-framework linkers, such as oligoynes[18] and oligothiophenes,[19] work as long-range molecular wires. These linkers are mostly composed of a carbon-based framework and other second row elements, while a heavier element-based framework has not yet been studied to the best of our knowledge.

Silicon is a heavier homolog of carbon and can form catenated systems called oligosilanes and polysilanes. These compounds are regarded as a pseudo one-dimensional molecular wire and have attracted much attention due to their unique photophysical and electronic properties,[20] as ascribed to the

† Present address: Department of Chimistry, Graduate School of Science, The University of Tokyo, 7-3-1 Hongo, Bunkyo-ku, Tokyo 113-0033

†† Present address: RIKEN Frontier Research System, 2-1 Hirosawa, Wako, Saitama 351-0198

Published on the web September 5, 2006; doi:10.1246/bcsj.79.1338

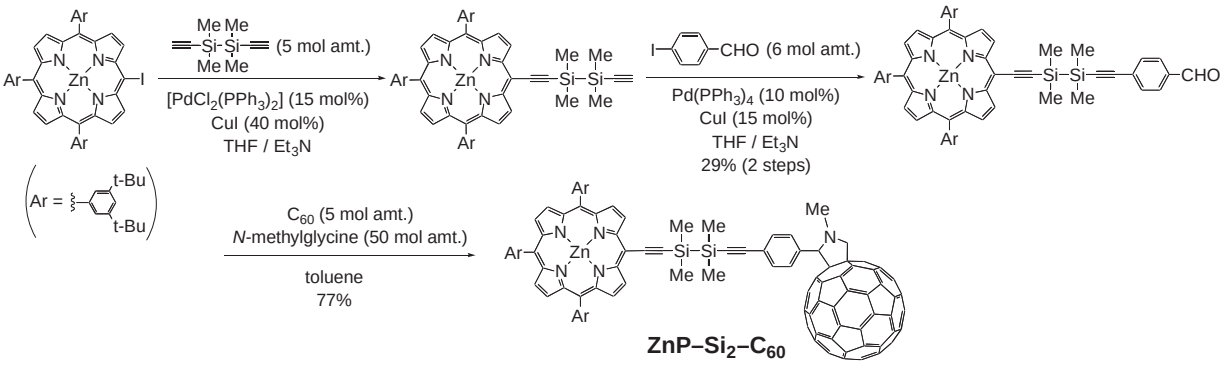

Scheme 1. Synthesis of the disilane-linked zinc porphyrin–fullerene dyad **Zn–Si$_2$–C$_{60}$**.

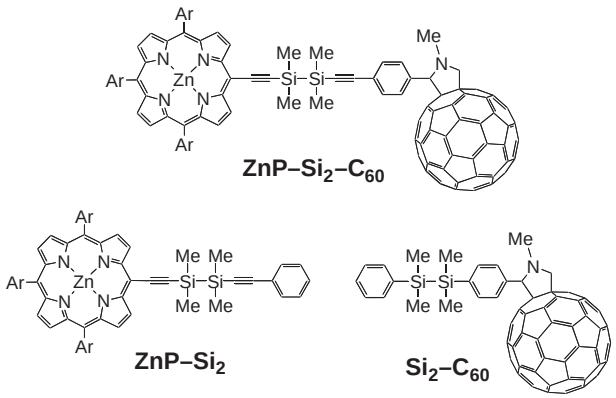

Chart 1. Structures of **ZnP–Si$_2$–C$_{60}$**, **ZnP–Si$_2$**, and **Si$_2$–C$_{60}$**.

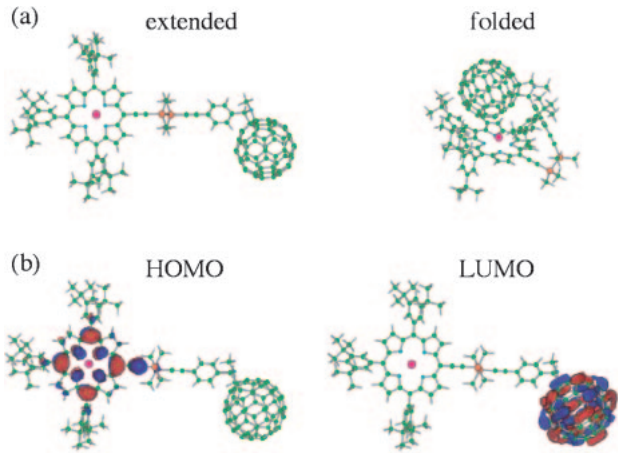

Fig. 1. (a) MM2 optimized structure of two possible conformers of **ZnP–Si$_2$–C$_{60}$**. (b) Frontier orbitals of the extended conformer based on B3LYP/6-31G calculations. Green = C, white = H, blue = N, orange = Si, and pink = Zn.

σ-electron delocalization over the silicon framework (σ-conjugation).[21] Construction of the porphyrin–fullerene-based intramolecular photoinduced ET system linked by a silicon chain is of interest in the light of the evaluation of the intramolecular ET ability along the σ-conjugated Si–Si bonds. Since such an ET system is unprecedented,[22–25] we now report the synthesis of the disilane-linked zinc porphyrin–fullerene dyad **ZnP–Si$_2$–C$_{60}$** (Chart 1) and its excited state dynamics on the basis of time-resolved absorption and fluorescence measurement studies.

Results and Discussion

Synthesis. The disilane-linked zinc porphyrin–fullerene dyad **ZnP–Si$_2$–C$_{60}$** was prepared as shown in Scheme 1. The zinc porphyrin (ZnP) and *p*-formylphenyl moieties were successively introduced into each end of the 1,2-diethynyl-1,1,2,2-tetramethyldisilane by Sonogashira coupling[26] followed by the Prato reaction[27] using *N*-methylglycine and C$_{60}$ to afford the target product **ZnP–Si$_2$–C$_{60}$**. The reference compound without the C$_{60}$ moiety, **ZnP–Si$_2$**, was prepared in a similar manner. The structures of these compounds synthesized in the present study were characterized by ^{1}H, ^{13}C, and ^{29}Si NMR and FAB mass spectra.

Conformer Considerations. The geometry optimization of **ZnP–Si$_2$–C$_{60}$** was performed by MM2 calculations. Two of the likely structures (extended and folded conformers) are shown in Fig. 1a, and the frontier molecular orbitals (MOs) of the extended conformer calculated using 6-31G basis set are shown in Fig. 1b. The HOMO and LUMO are localized at the ZnP moiety and the C$_{60}$ moiety, respectively. Although the HOMO orbitals delocalize over the ZnP and the alkyne moieties, the radical cation and the radical anion in the charge-separated state of the dyad are expected to mainly locate at the ZnP moiety and exclusively at the C$_{60}$ moiety, respectively. The center-to-center distances between these two radical-ion centers (R_{CC}) are evaluated to be 22.2 and 8.0 Å for the extended and the folded conformers, respectively.

In the ^{1}H NMR spectrum of **ZnP–Si$_2$–C$_{60}$**, the three sets of *tert*-butyl protons became magnetically unequivalent and are shifted downfield by 0.6 ppm at a maximum, whereas the β protons of the porphyrin ring are shifted upfield by 0.03–0.15 ppm as compared to those of **ZnP–Si$_2$**. The former phenomenon can be understood by the deshielding effect of the C$_{60}$ moiety in close proximity.[28] The latter case can also be explained by the shielding effect of the five-membered ring moiety of C$_{60}$[29] or the reduction in the ring current of the porphyrin ring by the attachment of an electron-withdrawing C$_{60}$.[30] Based on these results, the folded conformer should exist, but the ratio of the extended and folded conformers could not be determined due to the fast equilibrium between the conformers.

Electrochemistry Measurements. The oxidation potential (E_{ox}) and the reduction potential (E_{red}) of **ZnP–Si$_2$–C$_{60}$** were

Table 1. Free-Energy Change for Charge Separation from ^{1}ZnP*–Si$_2$–C$_{60}$ ($\Delta G_{CS(^1ZnP^*)}$), ZnP–Si$_2$–^{1}C$_{60}$* ($\Delta G_{CS(^1C_{60}^*)}$), ^{3}ZnP*–Si$_2$–C$_{60}$ ($\Delta G_{CS(^3ZnP^*)}$), and ZnP–Si$_2$–^{3}C$_{60}$* ($\Delta G_{CS(^3C_{60}^*)}$) and for Charge Recombination ($-\Delta G_{CR}$) to Ground State of **ZnP–Si$_2$–C$_{60}$**

Solvent	$-\Delta G_{CS(^1ZnP^*)}$ [a] /eV	$-\Delta G_{CS(^1C_{60}^*)}$ [a] /eV	$-\Delta G_{CS(^3ZnP^*)}$ [a] /eV	$-\Delta G_{CS(^3C_{60}^*)}$ [a] /eV	$-\Delta G_{CR}$ [a] /eV
THF	0.45	0.18	0.00	−0.07	1.57
BN	0.66	0.39	0.21	0.14	1.36

a) Calculated from Eqs. 1–3 using the following values: $\Delta E_{0\text{–}0} = 2.02$ eV for ^{1}ZnP*–Si$_2$–C$_{60}$; $\Delta E_{0\text{–}0} = 1.75$ eV for ZnP–Si$_2$–^{1}C$_{60}$*; $\Delta E_{0\text{–}0} = 1.57$ eV for ^{3}ZnP*–Si$_2$–C$_{60}$;[29] $\Delta E_{0\text{–}0} = 1.50$ eV for ZnP–Si$_2$–^{3}C$_{60}$*;[12,13,15,16] $E_{ox} = 0.34$ V and $E_{red} = -1.06$ V vs Fc/Fc$^+$ of ZnP–Si$_2$–C$_{60}$ in BN; the radii of the porphyrin ($R^+ = 4.8$ Å) and fullerene ($R^- = 4.7$ Å) and the center-to-center distance ($R_{CC} = 22.2$ Å) evaluated from Fig. 1; and permittivities of THF (7.58) and BN (25.2).

Table 2. UV–Vis–NIR Absorption and Fluorescence in BN of **ZnP–Si$_2$–C$_{60}$** and **ZnP–Si$_2$** at Room Temperature

Compound	Moiety	Absorption $\lambda_{A,max}$/nm ($\varepsilon/10^4$ M^{-1} cm^{-1})	Fluorescence λ_{em}/nm	ϕ [b]
ZnP–Si$_2$–C$_{60}$	ZnP	445 (27), 535 (0.5), 577 (1.2), 625 (1.6)	632, 684 (sh)	2.0×10^{-3}
	C$_{60}$	706 (0.04)	—[a]	—
ZnP–Si$_2$	ZnP	442 (52), 535 (0.5), 577 (1.7), 625 (2.5)	627, 681	7.3×10^{-2}

a) Not observed in BN. b) Fluorescence quantum yields of ZnP moiety of the dyad (ϕ_{dyad}) and the reference compound (ϕ_{ref}).

measured in benzonitrile (BN) using the square-wave voltammetry method in the presence of ferrocene as the internal standard. E_{ox} (+0.34 V vs Fc/Fc$^+$) and E_{red} (−1.06 V vs Fc/Fc$^+$) correspond to the first oxidation of the ZnP moiety and the first reduction of the C$_{60}$ moiety, respectively. From the observed E_{ox} and E_{red} values, the free-energy changes for the charge recombination (ΔG_{CR}) and the charge separation (ΔG_{CS}) can be calculated using the Weller's equations;[31]

$$-\Delta G_{CR} = e(E_{ox} - E_{red}) + \Delta G_S, \quad (1)$$

$$\Delta G_S = \frac{e^2}{4\pi\varepsilon_0}\left[\left(\frac{1}{2R^+} + \frac{1}{2R^-} - \frac{1}{R_{CC}}\right)\left(\frac{1}{\varepsilon_S}\right) - \left(\frac{1}{2R^+} + \frac{1}{2R^-}\right)\left(\frac{1}{\varepsilon_r}\right)\right], \quad (2)$$

$$-\Delta G_{CS} = \Delta E_{0\text{–}0} - (-\Delta G_{CR}), \quad (3)$$

where e and ε_0 are the elementary charge and vacuum permittivity, respectively; R^+ and R^- are the radii of the ion radicals of the ZnP and C$_{60}$ moiety, respectively; ε_S and ε_r are referred to as the static permittivity of the solvent used for the electrochemical measurement and that used for the spectroscopic measurements; $\Delta E_{0\text{–}0}$ is referred to as the energy of the 0–0 transition. The ΔG_{CS} and ΔG_{CR} values for **ZnP–Si$_2$–C$_{60}$** in THF and BN are summarized in Table 1. In polar solvents, the charge-separation (CS) processes via the excited singlet states of the ZnP moiety in **ZnP–Si$_2$–C$_{60}$** (^{1}ZnP*–Si$_2$–C$_{60}$) and the C$_{60}$ moiety (ZnP–Si$_2$–^{1}C$_{60}$*) are exothermic and are expected to occur. The CS process via the excited triplet states of the C$_{60}$ in **ZnP–Si$_2$–C$_{60}$** (ZnP–Si$_2$–^{3}C$_{60}$*) is slightly endothermic in THF and exothermic in BN. The CS would occur by a super-exchange mechanism via the disilane linkage on the basis of the relative orbital energy level of each component.

Steady-State Absorption. The steady-state absorption spectra of **ZnP–Si$_2$–C$_{60}$** (red line) and **ZnP–Si$_2$** (blue line) are shown in Fig. 2 together with that of **Si$_2$–C$_{60}$** (green line) in BN at room temperature. The representative absorption peaks ($\lambda_{A,max}$) are summarized in Table 2. The absorption peak of the Soret band of **ZnP–Si$_2$–C$_{60}$** ($\lambda_{A,max} = 445$ nm) showed a red-shift by 3 nm and the extinction coefficient was about half of that of **ZnP–Si$_2$**, whereas the absorption maximum wavelengths of the Q bands of **ZnP–Si$_2$–C$_{60}$** and **ZnP–Si$_2$** are essentially identical to each other. The spectrum of **ZnP–Si$_2$–C$_{60}$** slowly tails off up to 800 nm where the refer-

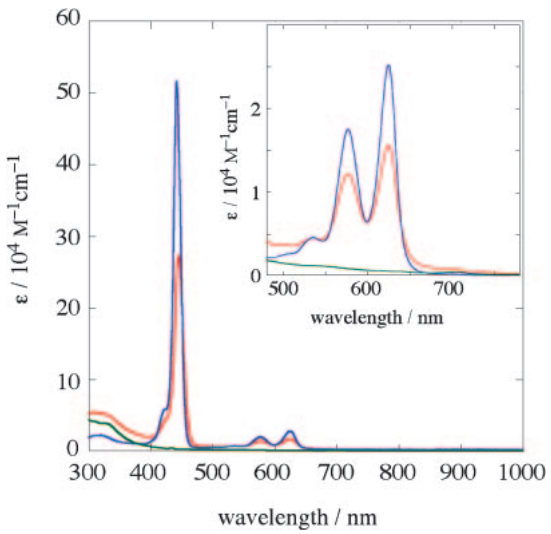

Fig. 2. UV–vis–NIR absorption spectra of **ZnP–Si$_2$–C$_{60}$** (red line), **ZnP–Si$_2$** (blue line), and **Si$_2$–C$_{60}$** (green line) in benzonitrile. Inset: Expanded spectra in the 480–780 nm region.

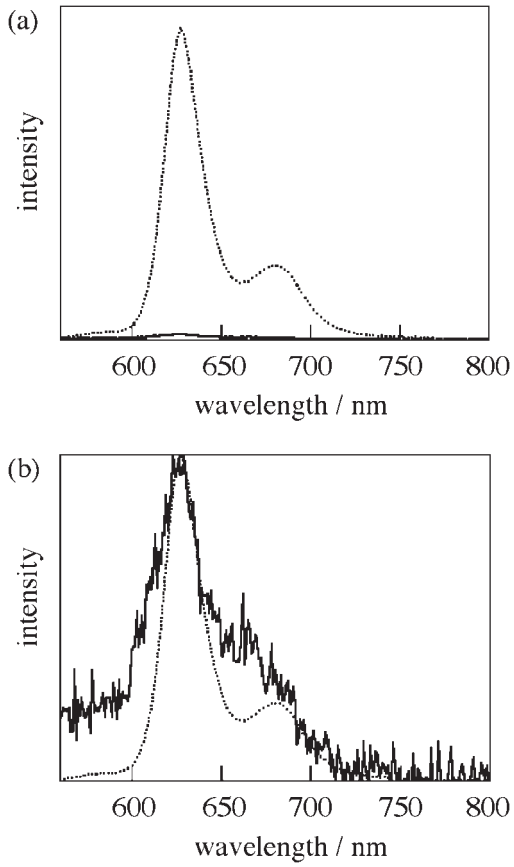

Fig. 3. Fluorescence spectra of **ZnP–Si$_2$–C$_{60}$** (solid line) and **ZnP–Si$_2$** (dotted line) in BN excited at 553 nm; (a) proportional to the fluorescence quantum yield and (b) normalized at a peak wavelength.

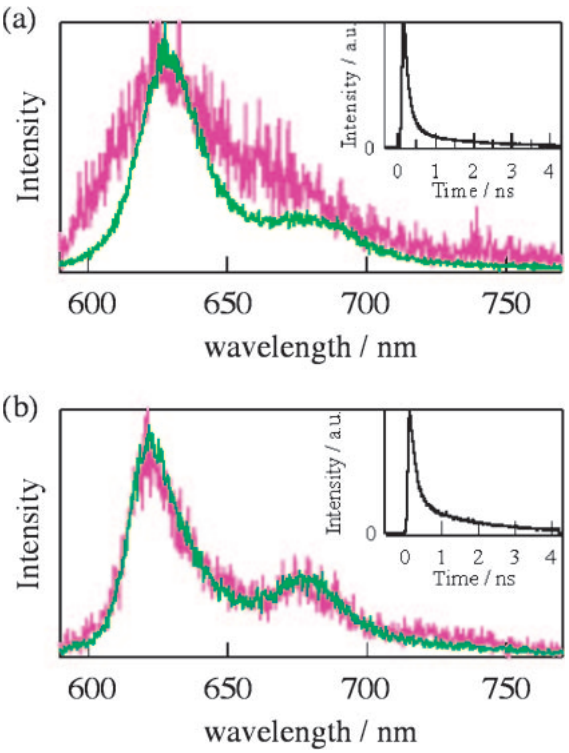

Fig. 4. Time-resolved fluorescence spectra of **ZnP–Si$_2$–C$_{60}$** in BN (a) and THF (b) at 0.1 ns (green line) and 1.0 ns (pink line) after excitation with 400 nm laser light, intensities are normalized at the peak. Inset: Fluorescence time-profile at the ZnP moiety.

ence compounds have no absorption. Similar absorption spectra were observed in other solvents such as THF. This band can be assigned to the CT absorption band of the folded conformer having an interaction between the ZnP- and the C_{60} moiety in the ground state due to the geometrical proximity of these two chromophores, which can directly form an exciplex by photoexcitation.[32] The variable temperature (VT) absorption spectra of **ZnP–Si$_2$–C$_{60}$** in toluene (Supporting Information) indicates increase in the interaction between ZnP and C_{60}; that is, the ratio of the folded conformer increases upon cooling even though the ratio cannot be precisely determined.

Steady-State and Time-Resolved Fluorescence and the Fluorescence Lifetime. Figure 3 shows the steady-state fluorescence spectra of **ZnP–Si$_2$–C$_{60}$** and **ZnP–Si$_2$** in BN with excitation at 553 nm, where the extinction coefficients of the two samples are equal. These results are summarized in Table 2. For the dyad, the fluorescence of the ZnP moiety (600–670 nm) was exclusively observed,[8,9,33] whereas that of the C_{60} moiety, normally appearing around 720 nm,[34] was hardly recognized. This observation is due to the spectral overlap with the shifted ZnP fluorescence and/or the CS from ZnP–Si$_2$–^{1}C$_{60}$* in BN. The relative fluorescence quantum yield of ^{1}ZnP* for **ZnP–Si$_2$–C$_{60}$** to **ZnP–Si$_2$**, based on the integration of the spectra from 560 to 750 nm, (ϕ_{dyad}/ϕ_{ref}) was evaluated to be 0.03 (Fig. 3a).

Figure 4 shows the time-resolved fluorescence spectra of **ZnP–Si$_2$–C$_{60}$** in THF and BN recorded with a time-correlated single-photon-counting apparatus with excitation at 400 nm. In all solvents, the initial fluorescence spectrum measured at 0.1 ns after the laser excitation was almost identical to that of **ZnP–Si$_2$**. In the spectrum at 1.0 ns, at which the fluorescence of the ZnP moiety had mostly disappeared, the fluorescence from the C_{60} moiety was hardly detected in the 700–750 nm region due to the low intensity.

Although the fluorescence decays of the ZnP moiety of **ZnP–Si$_2$–C$_{60}$** would consist of multicomponents as shown in the inset of Fig. 4, we analyzed the primary part using a single exponential fitting, which well reproduced the decay curve more than 80% of the entire time profile. The fluorescence lifetimes ($\tau_{F,dyad}$) of the ZnP moiety in BN and THF are summarized in Table 3, in which $\tau_{F,dyad}$ in toluene is also listed. The relative fluorescence quantum yield of the dyad to the reference compound **ZnP–Si$_2$** based on the fluorescence lifetimes ($\tau_{F,dyad}/\tau_{F,ref}$) was 0.08 in BN. This value is greater than that estimated from the steady-state fluorescence measurement ($\phi_{dyad}/\phi_{ref} = 0.03$). The difference between the two values also indicates the existence of the non-fluorescent folded conformer, and we can assign the observed emission mainly to the fluorescence of the extended conformer. This assignment is based on the assumption that the isomerization of the extended conformer to the folded conformer would be slow enough relative to the decay time scale of ^{1}ZnP*–Si$_2$–C$_{60}$, which is supported by the fluorescence lifetime measurements in frozen media (Supporting Information). The folded conformer, on the

Table 3. Fluorescence Lifetimes (τ_F), Quenching Rates ($k_q(^1ZnP^*)$, Quenching Quantum Yields ($\Phi_q(^1ZnP^*)$), and Rate Constant of Charge Recombination (k_{CR}), and Lifetime of Radical-Ion Pair (τ_{RIP})

Compound	Solvent	τ_F /ns (%)	$k_q(^1ZnP^*)$[a] /s^{-1}	$\Phi_q(^1ZnP^*)$[b]	k_{CR} /s^{-1}	τ_{RIP} /ns
ZnP–Si$_2$	Toluene	2.10 (100)	—	—	—	—
ZnP–Si$_2$–C$_{60}$	Toluene	0.23 (94)	3.8×10^9	0.89	—	—
	THF	0.19 (81)	4.8×10^9	0.91	1.9×10^6	520
	BN	0.16 (88)	5.8×10^9	0.92	2.3×10^6	430

a) $k_q(^1ZnP^*) = 1/\tau_{F,dyad} - 1/\tau_{F,ref}{}^{tol}$, where $\tau_{F,ref}{}^{tol}$ is the lifetime of **ZnP–Si$_2$** in toluene (2.10 ns). b) $\Phi_q(^1ZnP^*) = (1/\tau_{F,dyad} - 1/\tau_{F,ref}{}^{tol})/(1/\tau_{F,dyad})$.

other hand, would form the exciplex upon photoexcitation and its excited-state dynamics should be too fast for the present time scale. Thus, the origin of the observed quenching of $^1ZnP^*$–Si$_2$–C$_{60}$ in a polar solvent is based on the CS from the $^1ZnP^*$ moiety to the C$_{60}$ moiety (see transient absorption below). In a nonpolar solvent, fluorescence quenching is attributed to the CS via $^1ZnP^*$ followed by CR to $^1C_{60}^*$, which may be competitive to direct energy transfer to the ZnP–Si$_2$–$^1C_{60}^*$.[14] In polar solvents, the rates ($k_{CS}(^1ZnP^*)$) and the quantum yields ($\Phi_{CS}(^1ZnP^*)$) of the charge separation from $^1ZnP^*$–Si$_2$–C$_{60}$ were calculated to be equal to $k_q(^1ZnP^*)$ and $\Phi_q(^1ZnP^*)$ on assuming the predominant CS process (Table 3) according to the previous report.[14]

Transient Absorption Spectra. Figure 5a shows the nanosecond transient absorption spectra of **ZnP–Si$_2$–C$_{60}$** in BN measured at room temperature with an excitation wavelength at 532 nm, together with the time-profiles at 1000 nm in the Ar-saturated (red line) and O$_2$-saturated (black line) solutions in the inset. The absorption band around 1000 nm is characteristic of the $C_{60}^{\bullet-}$ species.[35] Although the absorption time profile at 1000 nm shows an apparent rise, this is due to the negative absorption by the scattered light. The other band in the 680–500 nm region is attributed to the $ZnP^{\bullet+}$ species,[36] which is partially hidden by the bleaching of the ground state-ZnP absorption in addition to the $^3ZnP^*$ and the $^3C_{60}^*$ absorptions. These spectral aspects unambiguously indicate the generation of the radical-ion pair ($ZnP^{\bullet+}$–Si$_2$–$C_{60}^{\bullet-}$) by photoinduced CS in a polar solvent such as BN. The absorption of the $C_{60}^{\bullet-}$ moiety in $ZnP^{\bullet+}$–Si$_2$–$C_{60}^{\bullet-}$ quickly disappeared in the O$_2$-saturated BN, which implies that $ZnP^{\bullet+}$–Si$_2$–$C_{60}^{\bullet-}$ reaches an equilibrium with ZnP–Si$_2$–$^3C_{60}^*$ and $^3ZnP^*$–Si$_2$–C$_{60}$ (the transient absorption spectra of these excited triplet states in toluene are shown in Supporting Information), because the reaction between the radical ions and O$_2$ was reported to be slow.[37] We assume that the equilibriums between the CS states and the triplet states are very fast while the decay of the triplet states is very slow, and therefore, the steady-state approximation can be applicable for the lifetime analysis of the radical-ion pair. Thus, the lifetime of the radical-ion pair (τ_{RIP}) was determined by single-exponential fitting to be 430 ns from the decay rate of the $C_{60}^{\bullet-}$ moiety (1000 nm) in **ZnP–Si$_2$–C$_{60}$** as shown in the inset of Fig. 5a. This single-exponential decay profile means that there is small spin coupling between these radical ion centers. The same decay rate was obtained by the decay time-profile analysis at 660 nm in a similar manner.

Figure 5b shows the transient absorption spectra of **ZnP–Si$_2$–C$_{60}$** in THF. The absorption bands of $ZnP^{\bullet+}$–Si$_2$–$C_{60}^{\bullet-}$

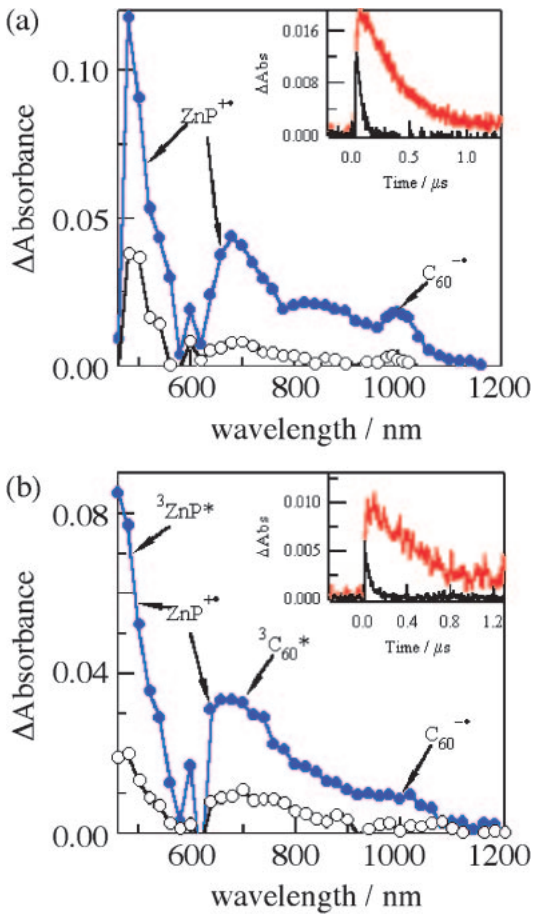

Fig. 5. Transient absorption spectra of **ZnP–Si$_2$–C$_{60}$** in BN (a) and THF (b) at 0.1 μs (blue-filled circle) and 1.0 μs (open circle) excited with 532 nm laser light at room temperature. Insets: Absorption time-profiles at 1000 nm under Ar-saturated solution (red line) and O$_2$-saturated solution (black line).

at 1000 and 650–700 nm are broadened as compared to those in BN. This broadening is due to the overlap of the absorption bands with those of the triplet species, $^3ZnP^*$–Si$_2$–C$_{60}$ and ZnP–Si$_2$–$^3C_{60}^*$, and indicates that the equilibrium between the charge-separated state and the excited triplet states shifts toward the latter in a less polar solvent. The lifetime of the radical ion pair τ_{RIP} in THF was estimated to be 520 ns based on the decay rate at 1000 nm since the absorption at 660 nm overlapped that of the triplet species. The slightly longer τ_{RIP} in THF than that in BN indicates that the charge recombination

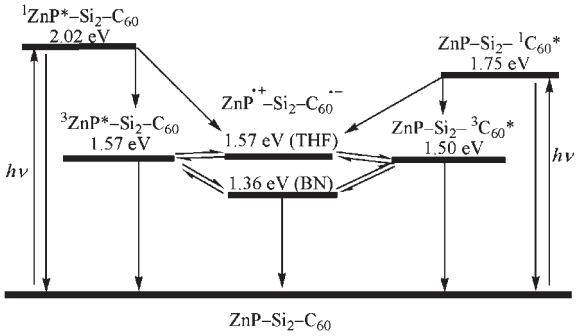

Scheme 2. The energy diagram of **ZnP–Si$_2$–C$_{60}$** on the basis of thermodynamic data and possible processes.

occurs in the Marcus inverted region; the large negative ΔG_{CR} value decreases the rate of the charge recombination.

Energy Diagrams. On the basis of the electrochemistry measurements, the Jabłoński diagram and the possible decay processes for the extended conformer of **ZnP–Si$_2$–C$_{60}$** were drawn (Scheme 2) although there must be other decay paths, such as isomerization to the folded conformer followed by the immediate formation of the non-emissive exciplex, which are not detectable on the present time scale. As demonstrated by the time-resolved absorption measurements, the CS from ^{1}ZnP*–Si$_2$–C$_{60}$ obviously occurs in polar solvents. However, clear-cut evidence of the CS from ZnP–Si$_2$–^{1}C$_{60}$* was not obtained from the spectroscopic studies although it is also possible in polar solvents based on the Jabłoński diagram. The lifetimes of the radical-ion pair ZnP$^{\bullet+}$–Si$_2$–C$_{60}^{\bullet-}$ in polar solvents are on the sub-microsecond order. The radical-ion pairs are in equilibrium with the excited triplet species as suggested by the transient absorption experiment in the O_2-saturated solution. The present decay sequences are qualitatively consistent with those determined for other porphyrin–fullerene dyads.[14,18,38]

Conclusion

A novel zinc porphyrin–fullerene dyad covalently connected by a disilane bridge (**ZnP–Si$_2$–C$_{60}$**) was synthesized and fully identified by its ^{1}H, ^{13}C, and ^{29}Si NMR and FAB mass spectra. The quenching paths from ^{1}ZnP*–Si$_2$–C$_{60}$ are most probably attributed to the charge separation in polar solvents. The transient absorption spectra in Ar-saturated polar solvents clearly show the formation of the radical ion pair. The dialkynyldisilane linkage plays an important role as a molecular wire, but the characteristic contribution of the silicon bridge to the photoexcited dynamics is not appreciable at the present stage. We are now designing longer multi-Si linkages to connect the ZnP and C$_{60}$ units as well as investigating the contribution of the conformational effect of the oligosilane linkage.

Experimental

General. ^{1}H and ^{13}C spectra were measured with JEOL EX-270 (270 MHz for ^{1}H and 67.94 MHz for ^{13}C) spectrometer or Varian Mercury (300 MHz for ^{1}H) in C_6D_6. Chemical shifts are reported in δ ppm with reference to internal solvent peak for ^{1}H (C_6HD_5: 7.20 ppm) and ^{13}C (C_6D_6: 128.0 ppm). ^{29}Si NMR spectra were recorded with JEOL EX-270 (59.62 MHz for ^{29}Si) spectrometer with the use of the proton-decoupled INEPT technique using tetramethylsilane (0.0 ppm) as an external standard. Mass spectra were performed at the Mass Spectrum Division of Institute for Chemical Research, Kyoto University. Recycle preparative gel permeation chromatography (GPC) was performed using polystyrene-gel columns (JAIGEL 1H and 2H, LC-908, Japan Analytical Industry) with toluene as an eluent. Thin-layer chromatography (TLC) was performed on plates coated with 0.25 mm thickness of silica gel 60F-254 (Merck). Column chromatography was performed by using Kieselgel 60 (70–230 mesh, Merck) unless otherwise stated. All reactions were carried out under nitrogen unless otherwise stated. Dry THF was freshly distilled from sodium/benzophenone under a nitrogen atmosphere before use.

Nanosecond transient absorption experiments were carried out using the 532 nm light from SHG of a Nd:YAG laser (Spectra-Physics, Quanta-Ray GCR-130, 6 ns fwhm) as an excitation source. Monitoring light from a pulsed Xe-lamp was detected with a Ge-APD detector in the near-IR region (600–1200 nm) and with a Si-PIN photodiode in the visible region (400–1000 nm). All the samples in a quartz cell (1 cm × 1 cm) were deaerated by bubbling argon gas through the solution for 15 min. The time-resolved fluorescence spectra were measured by a single photon counting method using a streakscope (Hamamatsu Photonics, C4334-01) equipped with a polychrometer and a SHG (400 nm) of a Ti:sapphire laser (Spectra-Physics, Tsunami 3950-L2S, 1.5 ps fwhm) as an excitation source. Steady-state absorption spectra were measured on a spectrophotometer (Jasco V570 DS). Steady-state fluorescence spectra were measured on a spectrofluorophotometer (Shimadzu RF-5300 PC). Osteryoung square wave voltammetry (OSWV) was carried out using a potentiostat (BAS, CV-50W) in a conventional three-electrode cell equipped with Pt working electrode, counter electrode, and an Ag/AgCl reference electrode in the presence of tetrabutylammonium perchlorate as an electrolyte at room temperature.

Synthesis. ZnP–Si$_2$–CHO: A solution of {5-iodo-10,15,20-tris[3,5-di(*t*-butyl)phenyl]porphinato}zinc(II)[39] (206 mg, 0.194 mmol) in THF (50 mL) was deoxygenized by bubbling with nitrogen for 30 min. To this solution were added 1,2-diethynyl-1,1,2,2-tetramethyldisilane (191 mg, 1.15 mmol), dichlorobis(triphenylphosphine)palladium(II) (21.4 mg, 0.0305 mmol), copper(I) iodide (14.9 mg, 0.0782 mmol), and triethylamine (1.0 mL, 7.17 mmol). After being stirred for 4 h at room temperature, the reaction mixture was evaporated, suspended in CH_2Cl_2, and filtered through a pad of silica gel (Wakogel 50C18). Evaporation gave 403 mg of a crude product as a purple solid.

A solution of thus prepared crude product (361 mg, 0.174 mmol) in THF (50 mL) was deoxygenized by bubbling with nitrogen for 30 min. To this solution were added *p*-iodobenzaldehyde (249 mg, 1.07 mmol), tetrakis(triphenylphosphine)palladium(0) (22.4 mg, 0.0194 mmol), copper(I) iodide (4.6 mg, 0.0242 mmol), and triethylamine (2.0 mL, 14.3 mmol). After being stirred for 12 h at room temperature, the reaction mixture was evaporated and suspended in CH_2Cl_2 and filtered through a pad of silica gel. After the evaporation, the residue was subjected to GPC (toluene as an eluent, $t_R = 74$ min). The collected fraction was evaporated and subjected to silica-gel column (hexane/toluene = 1/1, then 1/2) to give 61.2 mg (0.0507 mmol, 29% yield in 2 steps) of **ZnP–Si$_2$–CHO** as a purple solid. ^{1}H NMR (300 MHz) δ 0.74 (s, 6H), 0.86 (s, 6H), 1.53 (s, 18H), 1.56 (s, 36H), 7.39 (d, $J = 8.1$ Hz, 2H), 8.02 (t, $J = 1.8$ Hz, 1H), 8.05 (t, $J = 1.8$ Hz, 2H), 8.39–8.41 (m, 6H), 9.19–9.24 (m, 4H), 9.31–9.32 (m, 3H), 10.25 (d, $J = 4.5$ Hz, 2H). ^{13}C NMR (67.81 MHz) δ −2.33, −2.06, 32.03, 35.29, 35.32, 97.51, 98.40, 99.53, 107.68, 112.27, 121.16, 123.59, 124.69,

127.84, 129.14, 129.29, 130.17, 130.22, 131.19, 132.39, 132.44, 132.80, 133.43, 134.68, 135.72, 142.71, 142.88, 149.05, 149.08, 150.53, 150.61, 151.35, 153.03, 190.12. ^{29}Si NMR (53.67 MHz) δ −36.04, −35.47. HRMS(FAB): Calcd for $C_{77}H_{88}N_4OSi_2Zn$: 1204.5788. Found: 1204.5822.

ZnP–Si$_2$–C$_{60}$: A solution of **ZnP–Si$_2$–CHO** (30.6 mg, 0.0253 mmol), C_{60} (94.0 mg, 0.130 mmol), and *N*-methylglycine (115 mg, 1.28 mmol) in toluene (150 mL) was deoxygenized by bubbling with nitrogen for 30 min and heated under reflux. After being stirred for 12 h in the dark at this temperature, the reaction mixture was allowed to cool to room temperature and filtered through a pad of silica gel. After the evaporation, the residue was subjected to silica-gel column chromatography (hexane/toluene = 4/1, then 2/3). The collected fraction was evaporated and subjected to GPC (toluene as an eluent, t_R = 75 min) to give 38.1 mg (0.0195 mmol, 77% yield) of **ZnP–Si$_2$–C$_{60}$** as a dark purple solid. ^{1}H NMR (300 MHz) δ 0.70 (s, 3H), 0.73 (s, 3H), 0.76 (s, 6H), 1.58 (s, 18H), 1.59 (s, 18H), 1.62 (s, 18H), 2.45 (s, 3H), 3.03 (d, J = 9.6 Hz, 1H), 3.82 (s, 1H), 3.95 (d, J = 9.0 Hz, 1H), 7.45–7.48 (m, 2H), 7.70 (d, J = 8.7 Hz, 2H), 8.02 (t, J = 1.8 Hz, 1H), 8.04 (t, J = 1.7 Hz, 2H), 8.32–8.33 (m, 2H), 8.39 (m, 2H), 8.45–8.46 (m, 2H), 9.05 (d, J = 4.5 Hz, 2H), 9.12 (d, J = 4.5 Hz, 2H), 9.26 (d, J = 4.5 Hz, 2H), 10.15 (d, J = 4.5 Hz, 2H). ^{13}C NMR (67.81 MHz) δ −2.31, −2.21, −2.03, 32.17, 32.36, 35.39, 39.60, 68.22, 69.14, 76.46, 82.35, 93.72, 99.12, 99.94, 109.04, 111.40, 121.14, 123.52, 123.77, 124.84, 126.40, 127.21, 127.84, 128.18, 128.77, 128.92, 129.07, 129.27, 129.53, 130.11, 130.24, 130.32, 130.52, 131.32, 132.46, 133.00, 133.32, 133.79, 134.22, 134.30, 135.49, 135.67, 137.68, 137.91, 138.14, 138.63, 139.07, 139.19, 139.77, 139.95, 140.08, 140.14, 140.57, 140.77, 140.92, 141.21, 141.26, 141.30, 141.43, 141.48, 141.71, 141.82, 141.86, 142.04, 142.65, 142.73, 143.22, 143.42, 143.57, 143.73, 143.78, 144.06, 144.14, 144.29, 144.36, 144.41, 144.47, 144.64, 145.10, 145.18, 145.29, 145.39, 145.43, 145.48, 146.58, 149.05, 149.10, 150.28, 150.46, 151.15, 152.12, 152.19, 152.57, 152.88, 155.41. ^{29}Si NMR (53.67 MHz) δ −35.74, −35.69. FAB-MS: 1953 ($M + H^+$).

1-Ethynyl-1,1,2,2-tetramethyl-2-(phenyl)ethynyldisilane: To a solution of 1,2-dichloro-1,1,2,2-tetramethyldisilane (3.70 g, 19.8 mmol) in THF (20 mL) was added 18.5 mL (20.2 mmol) of a 1.09 M solution of phenylethynylmagnesium bromide in THF dropwise over 15 min at 0 °C. Upon completion of the addition, the reaction mixture was allowed to warm up to room temperature. After being stirred for 4 h, the resulting mixture was cooled to 0 °C. To this mixture was added 40 mL (20.0 mmol) of a 0.5 M solution of ethynylmagnesium chloride in THF dropwise over 20 min at 0 °C. Upon completion of the addition, the reaction mixture was allowed to warm to room temperature. After being stirred for 19 h, the resulting mixture was evaporated to remove THF. To the residue were added H_2O (50 mL) and Et_2O (50 mL). The resulting biphasic mixture was separated and the aqueous layer was extracted with Et_2O (4 × 50 mL). The combined organic layer was washed with brine (100 mL) and dried over $MgSO_4$. After filtration and evaporation, the residue was distilled under reduced pressure (bp 130–135 °C/8 mmHg) to give 3.54 g (14.6 mmol, 74% yield) of 1-ethynyl-1,1,2,2-tetramethyl-2-(phenyl)ethynyldisilane as a colorless oil. ^{1}H NMR (300 MHz) δ 0.41 (s, 6H), 0.46 (s, 6H), 2.20 (s, 1H), 6.94–6.96 (m, 3H), 7.47–7.50 (m, 2H). ^{13}C NMR (67.81 MHz) δ −2.82, −2.74, 92.03, 96.51, 108.71, 123.71, 128.48, 128.68, 132.13, 132.20. ^{29}Si NMR (53.67 MHz) δ −36.89, −36.19. HRMS(EI): Calcd for $C_{14}H_{18}Si_2$: 242.0947. Found: 242.0943.

ZnP–Si$_2$: A solution of {5-iodo-10,15,20-tris[3,5-di(*t*-butyl)-phenyl]porphinato}zinc(II) (102 mg, 0.0953 mmol) in THF (25 mL) was deoxygenized by bubbling with nitrogen for 30 min. To this solution were added 1-ethynyl-1,1,2,2-tetramethyl-2-(phenyl)ethynyldisilane (180.6 mg, 0.745 mmol), dichlorobis(triphenylphosphine)palladium(II) (11.4 mg, 0.0162 mmol), copper(I) iodide (8.6 mg, 0.0452 mmol), and triethylamine (0.5 mL, 3.59 mmol). After being stirred for 4 h at room temperature, the reaction mixture was evaporated, suspended in CH_2Cl_2, and filtered through a pad of silica gel. After evaporation, the residue was subjected to silica-gel column chromatography (hexane/toluene = 2/1, then 1/1). The collected fraction was evaporated and subjected to GPC (toluene as an eluent, t_R = 74 min) to give 52.2 mg (0.0443 mmol, 47% yield) of **ZnP–Si$_2$** as a purple solid. ^{1}H NMR (300 MHz) δ 0.76 (s, 6H), 0.87 (s, 6H), 1.52 (s, 18H), 1.56 (s, 36H), 6.93–6.95 (m, 3H), 7.02–7.06 (m, 2H), 7.50–7.53 (m, 2H), 7.59–7.62 (m, 2H), 8.01 (t, J = 1.8 Hz, 1H), 8.04 (t, J = 1.8 Hz, 2H), 8.39–8.40 (m, 4H), 8.41–8.42 (m, 2H), 9.20–9.24 (m, 4H), 9.29 (d, J = 4.8 Hz, 2H), 10.27 (d, J = 4.5 Hz, 2H). ^{13}C NMR (67.81 MHz) δ −2.14, −2.10, 31.95, 31.98, 35.26, 35.29, 92.92, 99.04, 100.06, 108.96, 111.73, 121.16, 123.48, 123.97, 124.48, 127.84, 128.18, 128.56, 128.79, 129.20, 130.11, 130.16, 131.41, 132.31, 132.38, 132.71, 133.41, 142.68, 142.84, 149.08, 150.51, 151.24, 153.09. ^{29}Si NMR (53.67 MHz) δ −36.04, −35.99. HRMS(FAB): Calcd for $C_{76}H_{88}N_4Si_2Zn$: 1176.5839. Found: 1176.5817.

Si$_2$–C$_{60}$: A solution of 1-(*p*-formylphenyl)-1,1,2,2-tetramethyl-2-phenyldisilane[40] (27.2 mg, 0.0911 mmol), C_{60} (324 mg, 0.449 mmol), and *N*-methylglycine (407 mg, 4.54 mmol) in toluene (400 mL) was deoxygenized by bubbling with nitrogen for 40 min and heated under reflux. After being stirred for 14 h in the dark at this temperature, the reaction mixture was allowed to cool to room temperature and filtered through a pad of silica gel. After the evaporation, the residue was subjected to silica-gel column chromatography (hexane/toluene = 4/1, then 1/1). The collected fraction was evaporated and subjected to GPC (toluene as an eluent, t_R = 100 min). After evaporation, the residue was washed with MeOH to give 39.9 mg (0.0381 mmol, 42% yield) of **Si$_2$–C$_{60}$** as a brown solid. ^{1}H NMR (300 MHz) δ 0.24 (s, 3H), 0.26 (s, 3H), 0.32 (s, 6H), 2.54 (s, 3H), 3.83 (d, J = 9.3 Hz, 1H), 4.51 (d, J = 9.3 Hz, 1H), 4.72 (s, 1H), 7.30–7.34 (m, 3H), 7.47 (d, J = 7.8 Hz, 2H), 7.7–7.8 (br, 2H). ^{13}C NMR (67.81 MHz) δ −3.99, −3.82, −3.77, 39.75, 69.44, 69.88, 77.80, 83.64, 128.82, 128.99, 134.15, 134.43, 136.11, 136.33, 136.87, 137.08, 137.86, 138.71, 139.67, 139.88, 140.18, 140.44, 140.49, 141.84, 141.97, 142.09, 142.28, 142.37, 142.43, 142.55, 142.61, 142.89, 143.01, 143.37, 143.50, 144.70, 144.88, 145.00, 145.44, 145.56, 145.69, 145.77, 145.82, 145.87, 146.00, 146.18, 146.36, 146.48, 146.53, 146.61, 146.76, 147.17, 147.53, 153.74, 154.02, 154.34, 156.73. ^{29}Si NMR (53.67 MHz) δ −21.77, −21.42. HRMS(FAB): Calcd for $C_{79}H_{27}NSi_2$: 1045.1682. Found: 1045.1709.

This work was supported by Grants-in-Aid for "Kyoto University Alliance for Chemistry," and "Giant Molecular Systems for Tohoku University." This work was also supported by Scientific Research on Priority Areas (No. 14078101, "Reaction Control of Dynamic Complexes" for HT and "Photofunctional Interface (417)") from the Ministry of Education, Culture, Sports, Science and Technology, Japan.

Supporting Information

VT steady-state absorption spectra of **ZnP–Si$_2$–C$_{60}$** in toluene, fluorescence lifetime measurements of **ZnP–Si$_2$–C$_{60}$** in frozen 2-methyltetrahydrofuran, and the nanosecond transient absorption

spectra in toluene solutions of **ZnP–Si$_2$** and **Si$_2$–C$_{60}$**. This material is available free of charge on the web at http://www.csj.jp/journals/bcsj/.

References

1 a) D. M. Guldi, *Chem. Soc. Rev.* **2002**, *31*, 22. b) H. Imahori, Y. Mori, Y. Matano, *J. Photochem. Photobiol., C* **2003**, *4*, 51.

2 For recent reviews: a) M. E. El-Khouly, O. Ito, P. M. Smith, F. D'Souza, *J. Photochem. Photobiol., C* **2004**, *5*, 79. b) H. Imahori, *Org. Biomol. Chem.* **2004**, *2*, 1425.

3 H. Imahori, Y. Sekiguchi, Y. Kashiwagi, T. Sato, Y. Araki, O. Ito, H. Yamada, S. Fukuzumi, *Chem. Eur. J.* **2004**, *10*, 3184.

4 A. Harriman, *Angew. Chem., Int. Ed.* **2004**, *43*, 4985.

5 a) M. R. Wasielewski, *Chem. Rev.* **1992**, *92*, 435. b) D. Gust, T. A. Moore, A. L. Moore, *Acc. Chem. Res.* **1993**, *26*, 198. c) A. Harriman, J. P. Sauvage, *Chem. Soc. Rev.* **1996**, *25*, 41. d) A. Osuka, N. Mataga, T. Okada, *Pure Appl. Chem.* **1997**, *69*, 797. e) D. Gust, T. A. Moore, *The Porphyrin Handbook*, ed. by K. M. Kadish, K. M. Smith, R. Guilard, Academic Press, San Diego, **2000**, Vol. 8, p. 153. f) D. Gust, T. A. Moore, A. L. Moore, *Acc. Chem. Res.* **2001**, *34*, 40. g) P. D. Harvey, *The Porphyrin Handbook*, ed. by K. M. Kadish, K. M. Smith, R. Guilard, Elsevier, **2003**, Vol. 18, p. 63. h) D. Kim, A. Osuka, *Acc. Chem. Res.* **2004**, *37*, 735.

6 a) H. Imahori, K. Hagiwara, T. Akiyama, S. Taniguchi, T. Okada, Y. Sakata, *Chem. Lett.* **1995**, 265. b) H. Imahori, K. Tamaki, H. Yamada, K. Yamada, Y. Sakata, Y. Nishimura, I. Yamazaki, M. Fujitsuka, O. Ito, *Carbon* **2000**, *38*, 1599.

7 a) P. Liddel, A. N. Macpherson, J. Sumida, L. Demanche, A. L. Moore, T. A. Moore, D. Gust, *Photochem. Photobiol.* **1994**, *59S*, 36S. b) D. Kuciauskas, S. Kin, G. R. Seely, A. L. Moore, T. A. Moore, D. Gust, T. Drovetskaya, C. A. Reed, P. D. W. Boyd, *J. Phys. Chem.* **1996**, *100*, 15926.

8 a) H. Imahori, Y. Sakata, *Adv. Mater.* **1997**, *9*, 537. b) D. Gust, T. A. Moore, A. L. Moore, *J. Photochem. Photobiol., B* **2000**, *58*, 63.

9 H. Imahori, K. Hagiwara, T. Akiyama, M. Aoki, S. Taniguchi, T. Okada, M. Shirakawa, Y. Sakata, *Chem. Phys. Lett.* **1996**, *263*, 545.

10 K. Ohkubo, H. Imahori, J. Shao, Z. Ou, K. M. Kadish, Y. Chen, G. Zheng, R. K. Pandey, M. Fujitsuka, O. Ito, S. Fukuzumi, *J. Phys. Chem. A* **2002**, *106*, 10991.

11 R. A. Marcus, *Angew. Chem., Int. Ed.* **1993**, *32*, 1111.

12 H. Imahori, H. Yamada, D. M. Guldi, Y. Endo, A. Shimomura, S. Kundu, K. Yamada, T. Okada, Y. Sakata, S. Fukuzumi, *Angew. Chem., Int. Ed.* **2002**, *41*, 2344.

13 H. Imahori, K. Hagiwara, M. Aoki, T. Akiyama, S. Taniguchi, T. Okada, M. Shirakawa, Y. Sakata, *J. Am. Chem. Soc.* **1996**, *118*, 11771.

14 H. Imahori, M. E. El-Khouly, M. Fujitsuka, O. Ito, Y. Sakata, S. Fukuzumi, *J. Phys. Chem. A* **2001**, *105*, 325.

15 A. S. D. Sandanayaka, K. Ikeshita, Y. Araki, N. Kihara, Y. Furusho, T. Takata, O. Ito, *J. Mater. Chem.* **2005**, *15*, 2276.

16 H. Imahori, K. Tamaki, Y. Araki, T. Hasobe, O. Ito, A. Shimomura, S. Kundu, T. Okada, Y. Sakata, S. Fukuzumi, *J. Phys. Chem. A* **2002**, *106*, 2803.

17 T. D. M. Bell, T. A. Smith, K. P. Ghiggino, M. G. Ranasinghe, M. J. Shephard, M. N. Paddon-Row, *Chem. Phys. Lett.* **1997**, *268*, 223.

18 a) K. Yamada, H. Imahori, Y. Nishimura, I. Yamazaki, Y. Sakata, *Chem. Lett.* **1999**, 895. b) A. Sato, K. Tashiro, K. Saigo, T. Aida, K. Yamanaka, M. Fujitsuka, O. Ito, 83rd Annual Meeting of the Chemical Society of Japan, Tokyo, March, **2003**, Abstr., No. 4C8-01. c) S. A. Vail, P. J. Krawczuk, D. M. Guldi, A. Palkar, L. Echegoyen, J. P. C. Tomé, M. A. Fazio, D. I. Schuster, *Chem. Eur. J.* **2005**, *11*, 3375.

19 a) J. Ikemoto, K. Takimiya, Y. Aso, T. Otsubo, M. Fujitsuka, O. Ito, *Org. Lett.* **2002**, *4*, 309. b) T. Nakamura, M. Fujitsuka, Y. Araki, O. Ito, J. Ikemoto, K. Takimiya, Y. Aso, T. Otsubo, *J. Phys. Chem. B* **2004**, *108*, 10700.

20 Reviews and accounts: a) M. Kumada, K. Tamao, *Adv. Organomet. Chem.* **1968**, *6*, 19. b) R. D. Miller, J. Michl, *Chem. Rev.* **1989**, *89*, 1359. c) R. West, *Comprehensive Organometallic Chemistry II*, ed. by E. W. Abel, F. G. A. Stone, G. Wilkinson, Pergamon, Oxford, **1995**, p. 77. d) M. Kira, T. Miyazawa, *The Chemistry of Organosilicon Compounds*, ed. by Z. Rappoport, Y. Apeloig, Wiley, Chichester, **1998**, Vol. 2, p. 1311. e) J. Michl, R. West, *Silicon-Containing Polymers*, ed. by R. G. Jones, W. Ando, J. Chojnowski, Kulwer Academic publishers, Dordrecht, **2000**, p. 499. f) R. West, *The Chemistry of Organosilicon Compounds*, ed. by Z. Rappoport, Y. Apeloig, Wiley, Chichester, **2001**, Vol. 3, p. 541. g) H. Tsuji, J. Michl, A. Toshimitsu, K. Tamao, *J. Synth. Org. Chem., Jpn.* **2002**, *60*, 762. h) H. Tsuji, J. Michl, K. Tamao, *J. Organomet. Chem.* **2003**, *685*, 9. i) Y. Hatanaka, *J. Organomet. Chem.* **2003**, *685*, 207.

21 Some recent reports on conformation dependence of oligosilane σ-conjugated system: a) B. Albinsson, H. Teramae, J. W. Downing, J. Michl, *Chem. Eur. J.* **1996**, *2*, 529. b) R. Imhof, H. Teramae, J. Michl, *Chem. Phys. Lett.* **1997**, *270*, 500. c) K. Obata, C. Kabuto, M. Kira, *J. Am. Chem. Soc.* **1997**, *119*, 11345. d) S. Mazières, M. K. Raymond, G. Raabe, A. Prodi, J. Michl, *J. Am. Chem. Soc.* **1997**, *119*, 6682. e) R. Tanaka, M. Unno, H. Matsumoto, *Chem. Lett.* **1999**, 595. f) K. Obata, M. Kira, *Organometallics* **1999**, *18*, 2216. g) I. El-Sayed, Y. Hatanaka, C. Muguruma, S. Shimada, M. Tanaka, N. Koga, M. Mikami, *J. Am. Chem. Soc.* **1999**, *121*, 5095. h) K. Tamao, H. Tsuji, M. Terada, M. Asahara, S. Yamaguchi, A. Toshimitsu, *Angew. Chem., Int. Ed.* **2000**, *39*, 3287. i) I. El-Sayed, Y. Hatanaka, S. Onozawa, M. Tanaka, *J. Am. Chem. Soc.* **2001**, *123*, 3597. j) H. Tsuji, A. Toshimitsu, K. Tamao, J. Michl, *J. Phys. Chem. A* **2001**, *105*, 10246. k) H. Tsuji, M. Terada, A. Toshimitsu, K. Tamao, *J. Am. Chem. Soc.* **2003**, *125*, 7486. l) H. Mallesha, H. Tsuji, K. Tamao, *Organometallics* **2004**, *23*, 1639. m) H. Tsuji, A. Fukazawa, S. Yamaguchi, A. Toshimitsu, K. Tamao, *Organometallics* **2004**, *23*, 3375. n) A. Fukazawa, H. Tsuji, K. Tamao, *J. Am. Chem. Soc.* **2006**, *128*, 6800.

22 For poly- or oligosilane–C$_{60}$ ET systems where the silicon moiety works as a donor: a) Y. Wang, R. West, C.-H. Yuan, *J. Am. Chem. Soc.* **1993**, *115*, 3844. b) R. G. Kepler, P. A. Cahill, *Appl. Phys. Lett.* **1993**, *63*, 1552. c) A. Watanabe, O. Ito, *J. Phys. Chem.* **1994**, *98*, 7736. d) K. Yoshino, K. Yoshimoto, M. Hamaguchi, T. Kawai, A. A. Zakhidov, H. Ueno, M. Kakimoto, H. Kojima, *Jpn. J. Appl. Phys.* **1995**, *34*, L141. e) Y. Sasaki, T. Konishi, M. Fujitsuka, O. Ito, Y. Maeda, T. Wakahara, T. Akasaka, M. Kako, Y. Nakadaira, *J. Organomet. Chem.* **2000**, *599*, 216. f) Y. Sasaki, M. Fujitsuka, O. Ito, Y. Maeda, T. Wakahara, T. Akasaka, K. Kobayashi, S. Nagase, M. Kako, Y. Nakadaira, *Heterocycles* **2001**, *54*, 777.

23 For a polysilane–porphyrin ET system where the silicon moiety works as a donor: Y. Matsui, K. Nishida, S. Seki, Y. Yoshida, S. Tagawa, K. Yamada, H. Imahori, Y. Sakata, *Organometallics* **2002**, *21*, 5144.

24 Recent studies on intramolecular ET between polysilane molecules: Y. Matsui, S. Seki, S. Tagawa, *Chem. Phys. Lett.* **2002**, *357*, 346.

25 An example of oligosilane-bridged dyads system where through-space energy transfer between the chromophores takes place: T. Karatsu, T. Shibata, A. Nishigaku, A. Kitamura, Y. Hatanaka, Y. Nishimura, S. Sato, I. Yamazaki, *J. Phys. Chem. B* **2003**, *107*, 12184.

26 K. Sonogashira, Y. Tohda, N. Hagihara, *Tetrahedron Lett.* **1975**, *50*, 4467.

27 M. Miggini, G. Scorrano, M. Prato, *J. Am. Chem. Soc.* **1993**, *115*, 9798.

28 For example: M. Prato, T. Suzuki, F. Wudl, V. Lucchini, M. Maggini, *J. Am. Chem. Soc.* **1993**, *115*, 7876.

29 For example: A. Pasquarello, M. Schlüter, R. C. Haddon, *Science* **1992**, *257*, 1660.

30 For example: W. J. Kruper, T. A. Chamberlin, M. Kochanny, *J. Org. Chem.* **1989**, *54*, 2753.

31 A. Weller, *Z. Phys. Chem.* **1982**, *132*, 93.

32 H. Imahori, N. V. Tkachenko, V. Vehmannen, K. Tamaki, H. Lemmetyinen, Y. Sakata, S. Fukuzumi, *J. Phys. Chem. A* **2001**, *105*, 1750.

33 H. Imahori, Y. Sakata, *Eur. J. Org. Chem.* **1999**, 2445.

34 D. M. Guldi, M. Prato, *Acc. Chem. Res.* **2000**, *33*, 1400.

35 a) M. A. Greaney, S. M. Gorun, *J. Phys. Chem.* **1991**, *95*, 7142. b) D. Dubois, K. M. Kadish, S. Flanagan, R. E. Haufler, L. B. F. Chibante, L. J. Willson, *J. Am. Chem. Soc.* **1991**, *113*, 4364. c) T. Kato, T. Kodama, T. Shida, T. Nakagawa, Y. Matsui, S. Suzuki, H. Shiromaru, K. Yamauchi, Y. Achiba, *Chem. Phys. Lett.* **1991**, *180*, 446.

36 a) J. H. Fuhrhop, D. Mauzerall, *J. Am. Chem. Soc.* **1969**, *91*, 4174. b) H. Chosrowjan, S. Tanigushi, T. Okada, S. Takagi, T. Arai, K. Tokumaru, *Chem. Phys. Lett.* **1995**, *242*, 644.

37 T. Konishi, M. Fujitsuka, O. Ito, *Chem. Lett.* **2000**, 202.

38 N. V. Tkachenko, L. Rantala, A. Y. Tauber, J. Helaja, P. H. Hynninen, H. Lemmetyinen, *J. Am. Chem. Soc.* **1999**, *121*, 9378.

39 F. Odobel, F. Suzenet, E. Blart, J.-P. Quintard, *Org. Lett.* **2000**, *2*, 131.

40 G. Mignani, A. Krämer, G. Pucetti, I. Ledoux, G. Soula, J. Zyss, *Mol. Eng.* **1991**, *1*, 11.